Semiconductor Physics, Quantum Electronics & Optoelectronics, 2015. V. 18, N 2. P. 188-192.
doi: 10.15407/spqeo18.02.188

PACS 77.80.Bh, 78.40.Ha

Temperature studies of optical parameters in $(Ag_3AsS_3)_{0.6}(As_2S_3)_{0.4}$ thin films

I.P. Studenyak[1], M.M. Kutsyk[1], Y.Y. Rati[1], V.Yu. Izai[1], S. Kökényesi[2], L. Daróci[2], R. Bohdan[2]
[1]*Uzhhorod National University, Faculty of Physics,*
3, Narodna Sq., 88000 Uzhhorod, Ukraine
[2]*Department of Experimental Physics, Faculty of Science and Technology, University of Debrecen,*
18/a Bem Sq., 4026 Debrecen, Hungary,
E-mail: studenyak@dr.com

Abstract. $(Ag_3AsS_3)_{0.6}(As_2S_3)_{0.4}$ thin films were deposited onto a silica substrate by using rapid thermal evaporation. The surfaces of the films were covered with Ag-rich crystalline micrometer-sized cones. The optical transmission spectra of thin films were studied within the temperature range 77…300 K. The absorption spectra in the region of its exponential behaviour were analysed, the dispersion dependences of refractive index as well as the temperature dependences of energy position of absorption edge and Urbach energy were investigated.

Keywords: thin film, thermal evaporation, optical absorption, Urbach energy, refractive index.

Manuscript received 02.12.14; revised version received 17.03.15; accepted for publication 27.05.15; published online 08.06.15.

1. Introduction

Among silver-containing chalcogenides, the Ag-As-S ternary system takes a remarkable place [1, 2]. Recently, we have reported about the structure [3], electrical conductivity [4], and optical absorption [5] in superionic Ag_3AsS_3–As_2S_3 glasses and composites. Thin films in this system, like to many other similar ones, were mostly prepared via deposition onto substrates using vacuum coating techniques, i.e. thermal evaporation, accompanied by a thermally or photo-induced dissolution of silver in As_2S_3 matrix [6, 7] or pulse laser deposition (PLD) [8]. A rather new method used is spin-coating technique [9, 10]. By the means of the PLD technique, a potentiometric thin film sensor can be realized on the basis of chalcogenide glasses (in particular Ag-As-S) [11].

In Ref. [12], we have presented the results of deposition of $(Ag_3AsS_3)_{0.6}(As_2S_3)_{0.4}$ thin films by using rapid thermal evaporation in vacuum. SEM and AFM imaging of the thin films revealed numerous micrometer-sized cones on their surfaces. The EDX analysis showed an excess of silver in the obtained cones, which, together with the pronounced peak of Ag in the XRD pattern, enabled us to ascribe the last one to the cones. The optical transmission spectra of the annealed and illuminated films have shown an increase of transmission, whereas the largest change of transmittance appeared to be a result of annealing at 50 °C and illumination for 1 min by the laser with the wavelength λ = 530 nm. It was shown that annealing and illumination lead to the increase in the energy position of the absorption edge, and to some decrease in the refractive index. In addition, it was revealed that annealing and illumination cause the Urbach energy decrease and, respectively, the decrease of structural disordering in the $(Ag_3AsS_3)_{0.6}(As_2S_3)_{0.4}$ thin films [12].

In this paper, we report on the temperature studies of optical absorption edge, investigations of temperature behaviour of the energy position of absorption edge, Urbach energy and refractive index as well as disordering processes in $(Ag_3AsS_3)_{0.6}(As_2S_3)_{0.4}$ thin film.

Semiconductor Physics, Quantum Electronics & Optoelectronics, 2015. V. 18, N 2. P. 188-192.
doi: 10.15407/spqeo18.02.188

2. Experimental

Synthesis of $(Ag_3AsS_3)_{0.6}(As_2S_3)_{0.4}$ composite material (which consists of crystalline Ag_3AsS_3 and glassy As_2S_3 [4]) was carried out at the temperature close to 700 °C for 24 h with subsequent melt homogenization for 72 h. $(Ag_3AsS_3)_{0.6}(As_2S_3)_{0.4}$ thin films were prepared by rapid thermal evaporation from the corresponding composite material at the temperature 1350 °C in vacuum ($3\cdot10^{-3}$ Pa) using a VU-2M setup. The composite material was initially placed in a tantalum evaporator, perforated for preventing the material falling out, on a glass substrate kept at room temperature. The film thickness was measured using an Ambios XP-1 profile meter.

Structural properties of the thin films under investigation were studied using SEM (Hitachi S-4300). It was shown the presence of cones on the top of a fresh evaporated thin films surface (Fig. 1). The average density of the cones on the surface of the thin films deposited at the evaporation temperature 1350 °C equals approximately 1.4×10^4 per mm^2. Energy-dispersive X-ray spectroscopy (EDX) was used to ascertain the thin film chemical composition. The composition of thin film has Ag content most close to initial bulk, since it is As-enriched and has a deficiency of sulphur [12].

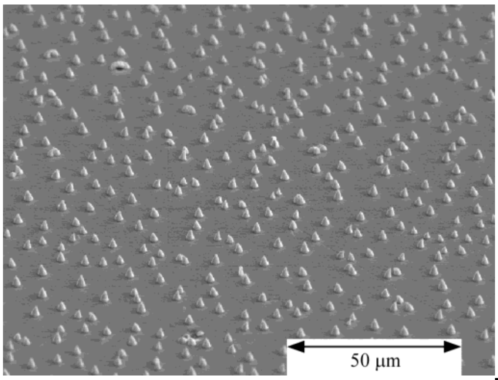

a

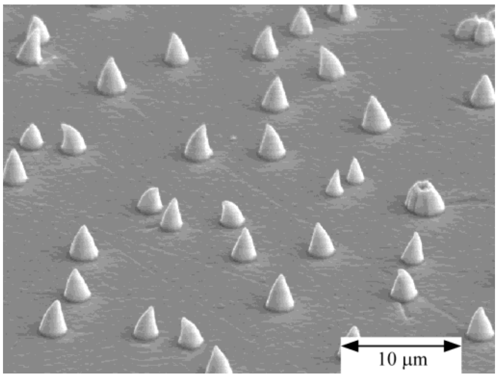

b

Fig. 1. Scaled SEM images of thermally evaporated $(Ag_3AsS_3)_{0.6}(As_2S_3)_{0.4}$ thin film.

Optical transmission spectra of $(Ag_3AsS_3)_{0.6}(As_2S_3)_{0.4}$ thin films were studied in the interval of temperatures 77…300 K by using the MDR-3 grating monochromator, a UTREX cryostat was used for low-temperature studies. From the temperature studies of interference transmission spectra, the spectral dependences of the absorption coefficient as well as dispersion dependences of the refractive index were derived [13].

3. Results and discussion

Interferential transmission spectra of $(Ag_3AsS_3)_{0.6}(As_2S_3)_{0.4}$ thin film at various temperatures within 77…300 K are shown in Fig. 2. With temperature, a red shift of both the shortwave part of the transmission spectrum (related to the temperature behaviour of the absorption edge) and the interferential maxima are observed. Besides, a typical decrease of transmission in the interferential maxima with temperature is revealed.

It is seen (Fig. 3) that the optical absorption edge spectra in the range of their exponential behaviour in $(Ag_3AsS_3)_{0.6}(As_2S_3)_{0.4}$ thin film, similarly to the bulk composite [5], are described by the Urbach rule [14]

$$\alpha(h\nu,T)=\alpha_0\cdot\exp\left[\frac{\sigma(h\nu-E_0)}{kT}\right]= =\alpha_0\cdot\exp\left[\frac{h\nu-E_0}{E_U(T)}\right], \quad (1)$$

where E_U is the Urbach energy (a reciprocal of the absorption edge slope $E_U^{-1}=\Delta(\ln\alpha)/\Delta(h\nu)$), σ is the absorption edge steepness parameter, α_0 and E_0 are the convergence point coordinates of the Urbach bundle. These coordinates α_0 and E_0 for the $(Ag_3AsS_3)_{0.6}(As_2S_3)_{0.4}$ thin film are given in Table.

Table. Parameters of Urbach absorption edge and EPI for $(Ag_3AsS_3)_{0.6}(As_2S_3)_{0.4}$ bulk composite and thin film.

Material	$(Ag_3AsS_3)_{0.6}$ $(As_2S_3)_{0.4}$ bulk composite	$(Ag_3AsS_3)_{0.6}$ $(As_2S_3)_{0.4}$ thin film
α_0 (cm^{-1})	$4.86\cdot10^7$	$3.2\cdot10^5$
E_0 (eV)	2.853	2.828
E_g^α (eV)	2.035	2.086
E_U (meV)	75.1	403
σ_0	0.514	0.106
$\hbar\omega_p$ (meV)	66.3	77.7
θ_E (K)	769	301
$(E_U)_0$ (meV)	64.5	360
$(E_U)_1$ (meV)	129.1	74.2
$E_g^\alpha(0)$ (eV)	2.158	2.165
S_g^α	21.9	5.27

Semiconductor Physics, Quantum Electronics & Optoelectronics, 2015. V. 18, N 2. P. 188-192.
doi: 10.15407/spqeo18.02.188

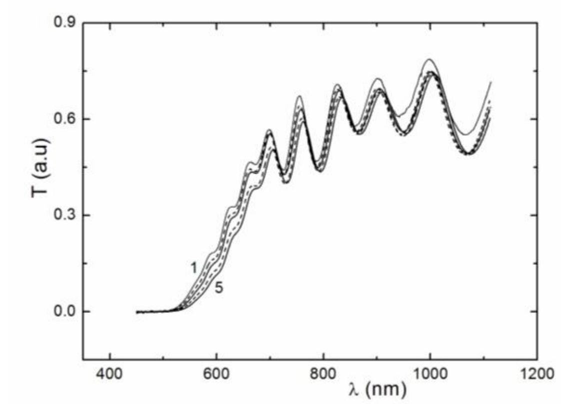

Fig. 2. Optical transmission spectra of $(Ag_3AsS_3)_{0.6}(As_2S_3)_{0.4}$ thin film at various temperatures: 77 (*1*), 150 (*2*), 200 (*3*), 250 (*4*) and 300 K (*5*).

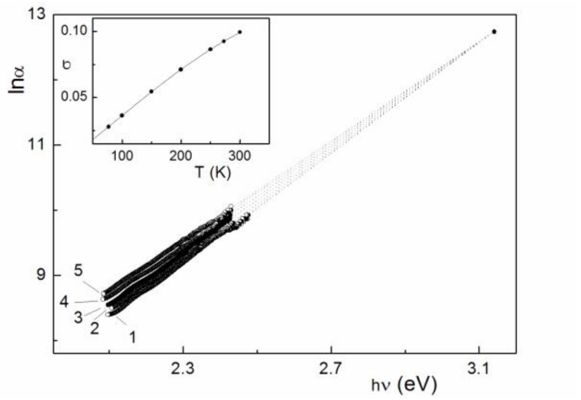

Fig. 3. Spectral dependences of the absorption coefficient of $(Ag_3AsS_3)_{0.6}(As_2S_3)_{0.4}$ thin film at various temperatures: 77 (*1*), 150 (*2*), 200 (*3*), 250 (*4*) and 300 K (*5*). The inset shows the temperature dependence of the steepness parameter σ.

The temperature behaviour of the Urbach absorption edge in $(Ag_3AsS_3)_{0.6}(As_2S_3)_{0.4}$ thin film is explained by electron-phonon interaction (EPI) that is strong in the film under investigation. The EPI parameters are obtained from the temperature dependence of absorption edge steepness parameter (Fig. 3) using the Mahr formula [15]

$$\sigma(T) = \sigma_0 \cdot \left(\frac{2kT}{\hbar\omega_p}\right) \cdot \tanh\left(\frac{\hbar\omega_p}{2kT}\right) \tag{2}$$

where $\hbar\omega_p$ is the effective phonon energy in the one-oscillator model, describing EPI, and σ_0 is the parameter related to the EPI constant g as $\sigma_0 = (2/3)g^{-1}$ (parameters $\hbar\omega_p$ and σ_0 are given in Table). For the $(Ag_3AsS_3)_{0.6}(As_2S_3)_{0.4}$ thin film $\sigma_0 < 1$, which is the evidence for strong EPI [16]. Besides, in the thin film, compared to the bulk composite, EPI is substantially enhanced (it corresponds to a decrease in the σ_0 parameter) and the energy $\hbar\omega_p$ of the effective phonon, taking part in absorption edge formation, increases (Table).

It should be noted that, in the range of exponential behaviour of optical absorption for their spectral characterization, one can use the energy position of an exponential absorption edge E_g^α at a fixed absorption coefficient α. Similarly to [12], we used the E_g^α values taken at $\alpha = 5\cdot10^4\,\text{cm}^{-1}$ for characterization of the absorption edge spectral position (Table). The temperature dependences of E_g^α and Urbach energy E_U for $(Ag_3AsS_3)_{0.6}(As_2S_3)_{0.4}$ thin film are presented in Fig. 4 and can be described in the Einstein model by relations [17, 18]

$$E_g^\alpha(T) = E_g^\alpha(0) - S_g^\alpha k\theta_E\left[\frac{1}{\exp(\theta_E/T) \ -1}\right], \tag{3}$$

$$E_U(T) = (E_U)_0 + (E_U)_1\left[\frac{1}{\exp(\theta_E/T) \ -1}\right], \tag{4}$$

where $E_g^\alpha(0)$ and S_g^α are the energy position of absorption edge at 0 K and a dimensionless constant, respectively; θ_E is the Einstein temperature, corresponding to the average frequency of phonon excitations of a system of non-coupled oscillators, $(E_U)_0$ and $(E_U)_1$ are constants. The obtained $E_g^\alpha(0)$, S_g^α, θ_E, $(E_U)_0$, and $(E_U)_1$ parameters for the thin film are given in Table, and the temperature dependences of E_g^α and the Urbach energy E_U for $(Ag_3AsS_3)_{0.6}(As_2S_3)_{0.4}$ thin film calculated from Eqs. (3) and (4) are shown in Fig. 4 as solid and dashed lines, respectively.

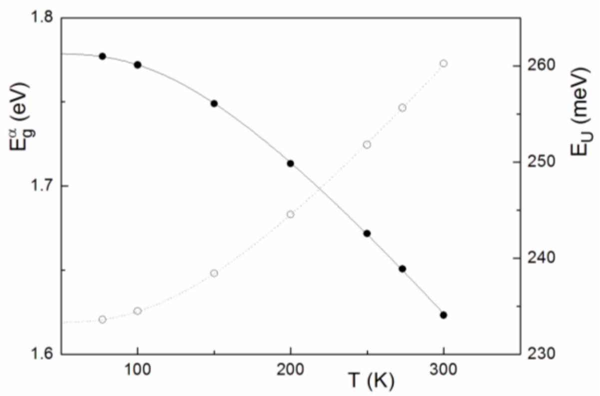

Fig. 4. Temperature dependences of the absorption edge energy position E_g^α ($\alpha = 5\cdot10^4\,\text{cm}^{-1}$) (*1*) and Urbach energy E_U (*2*) of $(Ag_3AsS_3)_{0.6}(As_2S_3)_{0.4}$ thin film.

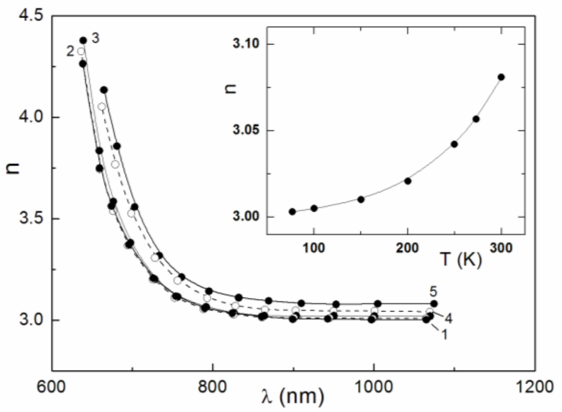

Fig. 5. Refractive index dispersions of $(Ag_3AsS_3)_{0.6}(As_2S_3)_{0.4}$ thin film at various temperatures: 77 (*1*), 150 (*2*), 200 (*3*), 250 (*4*) and 300 K (*5*). The inset shows the temperature dependence of the refractive index.

An essential characteristic of the absorption edge spectra of the thin film under investigation is a lengthy Urbach tail, which results in the Urbach energy E_U being more than five times higher than that in the bulk composite. In Ref. [19], it was shown that temperature, structural and compositional disordering affect the Urbach absorption edge shape, i.e. the Urbach energy E_U is described by the equation

$$E_U = (E_U)_T + (E_U)_X + (E_U)_C = (E_U)_T + (E_U)_{X+C}, \quad (5)$$

where $(E_U)_T$, $(E_U)_X$ and $(E_U)_C$ are contributions of temperature, structural and compositional disordering to E_U, respectively. It should be noted that the first term in the right-hand side of Eq. (4) represents the sum of structural and compositional disordering, and the second one represents temperature disordering.

It is worth to note that the absolute value of the contribution of structural disordering into the film Urbach energy at the fixed value of the contribution of compositional disordering ($x = 0.6$) increases by factor higher than 5 in comparison with the bulk composite. Structural disordering in $(Ag_3AsS_3)_{0.6}(As_2S_3)_{0.4}$ thin film may be increased due to: (1) the absence of long-range order in the atomic arrangement and chemical bond breakdown; (2) the lower density of the atomic structure package due to the presence of pores; (3) the transition from the three-dimensional bulk structure to the two-dimensional planar structure.

The dispersion dependences of the refractive index for the as-deposited thin films were obtained from the interference transmission spectra (Fig. 5). The slight dispersion of the refractive index is observed in the transparency region while it increases when approaching to the optical absorption edge region. With temperature growth, the nonlinear increase of refractive index in $(Ag_3AsS_3)_{0.6}(As_2S_3)_{0.4}$ thin film is revealed.

4. Conclusions

$(Ag_3AsS_3)_{0.6}(As_2S_3)_{0.4}$ thin films were deposited onto a silica substrate by using rapid thermal evaporation. SEM imaging of the thin films revealed numerous micrometer-sized Ag-containing cones on their surfaces. The spectral dependences of the absorption coefficient as well as dispersion dependences of the refractive index were derived from the spectrometric studies of interference transmission spectra. In the range of the exponential behaviour of the optical absorption edge, the energy position of exponential absorption edge E_g^{α} and the Urbach energy E_U in $(Ag_3AsS_3)_{0.6}(As_2S_3)_{0.4}$ thin film have been determined. Temperature variation of the transmission spectra as well as temperature behaviour of the absorption edge spectra in the range of its exponential tail have been studied. A typical Urbach bundle is observed, temperature dependences of the absorption edge the energy position and the Urbach energy have been obtained. The influence of different type of disordering on the Urbach tail has been studied, and a comparative analysis of the Urbach absorption edge parameters for $(Ag_3AsS_3)_{0.6}(As_2S_3)_{0.4}$ bulk composite and thin film has been performed.

References

1. R.E. Belford, E. Hajto, A.E. Owen, The selective removal of the negative high-resolution photoresist system Ag-As-S // *Thin Solid Films*, **173**, p. 129-137 (1989).
2. M.N. Kozicki, M. Mitkova, Mass transport in chalcogenide electrolyte films – materials and applications // *J. Non-Cryst. Solids*, **352**, p. 567-577 (2006).
3. I. Studenyak, Yu. Neimet, C. Cserhati, S. Kökényesi, E. Kazakevičius, T. Šalkus, A. Kežionis, A. Orliukas, Structural and electrical investigations of $(Ag_3AsS_3)_x(As_2S_3)_{1-x}$ superionic glasses // *Cent. Eur. J. Phys.* **10**, p. 206-209 (2012).
4. I.P. Studenyak, Yu.Yu. Neimet, M. Kranjčec, A.M. Solomon, A.F. Orliukas, A. Kežionis, E. Kazakevičius, T. Šalkus, Electrical conductivity studies in $(Ag_3AsS_3)_x(As_2S_3)_{1-x}$ superionic glasses and composites // *J. Appl. Phys.* **115**, 033702-1−033702-5 (2014).
5. I.P. Studenyak, M. Kranjcec, Yu.Yu. Neimet, M.M. Pop, Optical absorption edge in $(Ag_3AsS_3)_x(As_2S_3)_{1-x}$ superionic glasses // *Semiconductor Physics, Quantum Electronics & Optoelectronics*, **15**(2), p. 147-151 (2012).
6. T. Wagner, V. Perina, A. Mackov, E. Rauhala, A. Seppala, Mir. Vlcek, S.O. Kasap, Mil. Vlcek, M. Frumar, The tailoring of the composition of Ag–As–S amorphous films using photo-induced solid state reaction between Ag and $As_{30}S_{70}$ films // *Solid State Ionics*, **141–142**, p. 387-395 (2001).

7. A. Kovalskiy, H. Jain, M. Mitkova, Evolution of chemical structure during silver photodiffusion into chalcogenide glass thin films // *J. Non-Cryst. Solids*, **355**, p. 1924-1929 (2009).
8. P. Nemec, M. Frumar, J. Jedelsky, M. Jelınek, J. Lancok, I. Gregora, Thin amorphous chalcogenide films prepared by pulsed laser deposition // *J. Non-Cryst. Solids*, **299-302**, p. 1013-1017 (2002).
9. T. Wagner, T. Kohoutek, Mir. Vlcek, Mil. Vlcek, M. Munzar, M. Frumar, Spin-coated $Ag_x(As_{0.33}S_{0.67})_{100-x}$ films: preparation and structure // *J. Non-Cryst. Solids*, **326-327**, p. 165-169 (2003).
10. T. Kohoutek, T. Wagner, J. Orava, M. Frumar, V. Perina, A. Mackova, V. Hnatowitz, M. Vlcek, S. Kasap, Amorphous films of Ag–As–S system prepared by spin-coating technique, preparation techniques and films physico-chemical properties // *Vacuum*, **76**, p. 191-194 (2004).
11. M.J. Schoening, C. Schmidt, J. Schubert et al., Thin films on the basis of chalcogenide glass materials prepared by pulsed laser deposition technique // *Sensors and Actuators B*, **68**, p. 254-259 (2000).
12. I.P. Studenyak, Yu.Yu. Neimet, Y.Y. Rati, D. Stanko, M. Kranjčec, S. Kökényesi, L. Daróci, R. Bohdan, Structural and optical properties of annealed and illuminated $(Ag_3AsS_3)_{0.6}(As_2S_3)_{0.4}$ thin films // *Opt. Mat.* **37**, p. 718-723 (2014).
13. R. Swanepoel, Determination of the thickness and optical constants of amorphous silicon // *J. Phys. E: Sci. Instrum.* **16**, p. 1214-1222 (1983).
14. F. Urbach, The long-wavelength edge of photographic sensitivity and of the electronic absorption of solids // *Phys. Rev*. **92**, p. 1324-1326 (1953).
15. H. Sumi, A. Sumi, The Urbach-Martienssen rule revisited // *J. Phys. Soc. Jpn.* **56**, p. 2211-2220 (1987).
16. M.V. Kurik, Urbach rule (Review) // *phys. status solidi* (*a*), **8**, p. 9-30 (1971).
17. M. Beaudoin, A.J.G. DeVries, S.R. Johnson, H. Laman, T. Tiedje, Optical absorption edge of semi-insulating GaAs and InP at high temperatures // *Appl. Phys. Lett.* **70**, p. 3540-3542 (1997).
18. Z. Yang, K.P. Homewood, M.S. Finney, M.A. Harry, K.J. Reeson, Optical absorption study of ion beam synthesized polycrystalline semiconducting $FeSi_2$ // *J. Appl. Phys.***78**, p. 1958-1963 (1995).
19. G.D. Cody, T. Tiedje, B. Abeles, B. Brooks, Y. Goldstein, Disorder and the optical-absorption edge of hydrogenated amorphous silicon // *Phys. Rev. Lett.* **47**, p. 1480-1483 (1981).